e-ISSN: 277<u>6-2521</u>



I CPES

Journal of Computation Physics and Earth Science Volume 1 No. 2 October, 2021



Email:
adm.jocpes@gmail.com
admin@physan.org

https://journal.physan.org/index.php/jocpes

ISSN: 2776-2521 (online)

Volume 1, Number 2, October 2021, Page 32-36 https://journal.physan.org/index.php/jocpes/index

32

Active Tectonic Segmentation on the Micro Plate of Northern Sumatra Based on Distribution of Earthquake Epicenter in July 2020

Nesia Sabrina Marbun¹, Melda Panjaitan², Triya Fachriyeni³, Eridawati⁴

^{1, 3, 4}Indonesian Agency for Meteorological, Climatological and Geophysics ²Department of Computer Science, Universitas Budi Darma

Article Info

Article history:

Received September 12, 2021 Revised September 24, 2021 Accepted October 01, 2021

Keywords:

Earthquake activity, Segmentation, Fault.

ABSTRACT

The main goal of this study to increase awareness of earthquake activity due to local faults that have so far received "less attention". Continuous observations can be made on site (on active faults), by using portable seismographs and/or by utilizing the Indonesia Tsunami Early Warning System (Ina-TEWS) network broadband sensors adjacent to these active faults. However, observing using a Portable Seismograph for a long period of time will certainly require a large amount of money. Therefore, it will be more effective to utilize data from seismic sensors that are relatively close to the suspected faults. Based on the analysis that has been carried out, it can be concluded that, in the period from July 1, 2020 to July 31, 2020, there have been 79 earthquakes in the North Sumatra region, with magnitudes between 2.0 - 5.2. The location of the earthquake was dominated by land earthquakes with shallow depths, namely 0-60 km with 54 events and at sea 25 occurrences. The most earthquake occurrences in the period 01 July 2020 - 31 July 2020 occurred around Cluster 1 (local fault Aceh Central, Batee-A, Aceh South, Pidie Jaya and Lot Aceh North, Seulimeum-South), namely 15 earthquake events, so it is classified as a cluster. which is very active in the July 2020 period. In the July 2020 period, seismic activity around the Tripa 2 and Oreng local faults was low compared to other local faults in Northern Sumatra, while in June 2020 there was no seismic activity around the Tripa local faults. 2, and the Oreng fault.

This is an open access article under the CC BY-SA license.



Corresponden Author:

Nesia Sabrina Marbun,

Badan Meteorologi Klimatologi dan Geofisika, Indonesia

Email: ziaraboen@gmail.com

1. INTRODUCTION

The Sumatran subduction belt is the line where the Indo-Australian Plate subducts under the Eurasian Plate. The Indo-Australian plate is moving northward at a speed relative to the Eurasian plate of 5-6 cm/year [1]–[5]. This causes the island of Sumatra to have two geological conditions that can affect seismic activity and the tectonic conditions of the island of Sumatra. First, the subduction zone which is the boundary between the Indian-Australian plate which dips into the Eurasian plate. This zone has the potential to cause an earthquake with a relatively larger magnitude so it is very likely to cause a tsunami [6]. Second, the Sumatran fault zone, also known as the Sumatra Fault Zone (SFZ) divides the island of Sumatra into two, stretching along the Bukit Barisan mountains, from the Andaman Sea to the Semangko Bay [7]–[9]. These two zones make the island of Sumatra very vulnerable to earthquakes. The distribution of seismicity and tectonic review in an area can be viewed qualitatively using statistical methods, so that the level of earthquake activity can be known [10], [11]. The purpose of this study is to increase awareness of earthquake activity due to local faults that have so far received "less attention". Continuous observations can be made on site (on active faults), by using portable seismographs and/or by utilizing the InaTEWS network broadband sensors adjacent to these

active faults. However, observing using a Portable Seismograph for a long period of time will certainly require a large amount of money. Therefore, it will be more effective to utilize data from seismic sensors that are relatively close to the suspected faults.

2. DATA AND METHOD

Earthquake record data is very useful because it can provide information on the subsurface geological structure as well as the level of tectonic activity. With one (or more) major earthquake accompanied by many aftershocks, we expect new and better information. In this study, data was collected from the recording of the InaTEWS seismograph sensor network and the results of earthquake analysis using the Seiscomp3 Deli Serdang Geophysical Station in the northern Sumatra region for a period of 1 month from July 1, 2020 to July 31, 2020 in order to display the state of regional tectonic activity. The selected earthquake events are earthquakes with a magnitude <5 SR and are classified based on the range of Magnitude M < 3.0; 3.0 \le M < 4; and 4 \le M < 5.

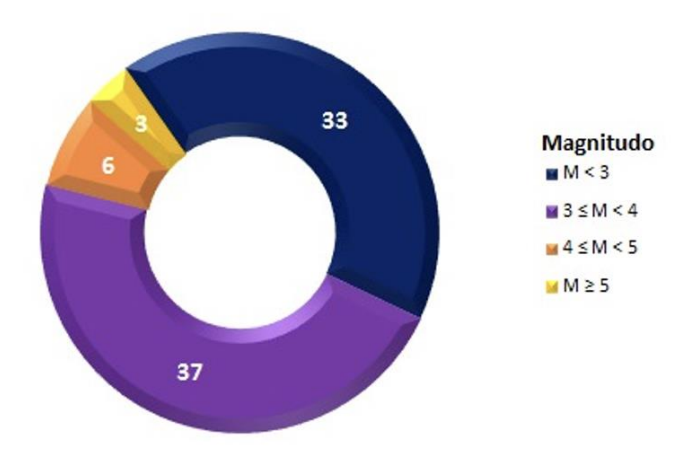


Fig. 1. Diagram of the number of earthquakes by magnitude in the North Sumatra Province July 1, 2020 to July 31, 2020

The high level of seismicity in the North Sumatra region is caused by the subduction of the Indo-Australian Plate which subducts under the Eurasian Plate to the west of Sumatra Island and the large fault of Sumatra Island. Micro-earthquakes recorded in the North Sumatra Province for a period of 1 month from July 1, 2020 to July 31, 2020 were 79 events. With the number of earthquakes M < 3.0 as many as 33 events, 3 \leq M \leq 4 as many as 37 events, for earthquakes $M \leq$ 5 as many as 6 events, and earthquakes $M \geq$ 5 as many as 3 events as shown in Figure 1.

3. RESULT AND DISCUSSION

Based on data from the 2017 Indonesia Earthquake Source and Hazard Map from the National Earthquake Study Center Team and research results [7] and summarized in the book on the tectonic face of Northern Sumatra [6]. North Sumatra province is crossed by several faults. Some of these faults have been identified and several parameters are known, such as sliprate and Mmax value.



Fig. 2. Earthquake clusters in Northern Sumatra in July 2020

Seismicity data due to fault activity in Northern Sumatra from July 1, 2020 to July 31, 2020 is shown in Figure 2. The criteria for determining earthquakes due to fault activity here are that the earthquake occurred on land, the depth was less than 30 km and the magnitude was less than 5. From the seismic data, it can be identified 5 clusters of earthquake sources due to fault activity in Northern Sumatra and its surroundings.

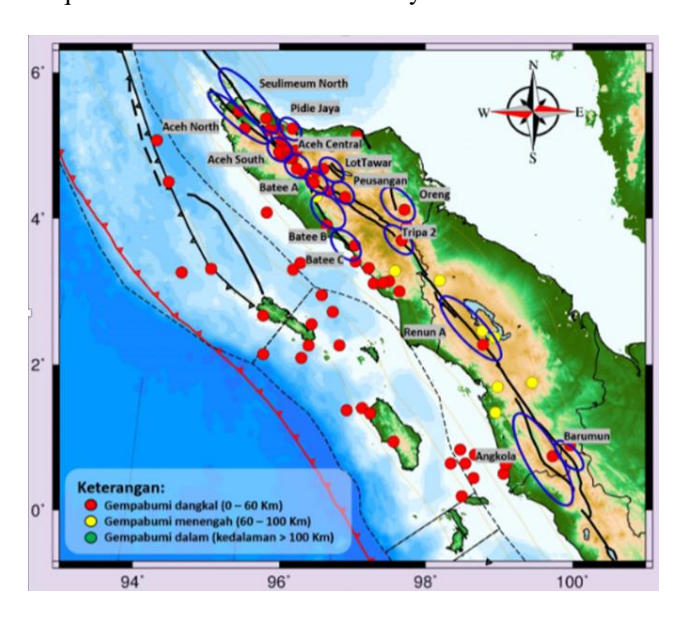


Fig. 3. Seismicity map segmentation due to fault activity in Northern Sumatra 1 July 2020 to 31 July 2020

The results of seismic segmentation of fault activity in the North Sumatra region for the period 1 to 31 July 2020 can be seen in Figure 4. The dominance of the Aceh Central segment/fault in July 2020 occurred 12 times. Based on clusters for the Northern Sumatra region, the results of segmentation or clusters describe Cluster 1 (Aceh North, Seulimeum-South) Judging from the location and depth of the hypocenter, the earthquakes in this area include shallow earthquakes which are thought to be the result of local fault activity in Aceh North and Seulimeum-South which causes rock deformation, thus triggering an earthquake. In the period Journal of Computation Physics and Earth Science Vol. 1, No. 2, October 2021: 32-36

01 July 2020 to 31 July 2020, 15 earthquakes occurred in this fault segment. In cluster 2 (Aceh Central, Batee-A, Aceh South, Pidie Jaya, Lot Tawar), Judging from the location and depth of the hypocenter, the earthquakes in this area include shallow earthquakes which are thought to be the result of local fault activity in Aceh Central, Batee-A, Aceh South, Pidie Jaya and Lot Tawar which caused rock deformation, thus triggering an earthquake. In the period 01 July 2020 to 31 July 2020, 9 earthquakes occurred in this fault segment. In cluster 3 (Tripa-2, Oreng fault), Judging from the location and depth of the hypocenter, the earthquakes in this area include shallow earthquakes which are thought to be the result of the local Tripa-2 fault and the Oreng fault which caused rock deformation, thus triggering an earthquake. In the period from July 1, 2020 to July 31, 2020, there were 3 earthquakes in this fault segment. In Cluster 4 (Renun-A), judging from the location and depth of the hypocenter, the earthquakes in this area include shallow earthquakes which are thought to be the result of the local faults of Barumun and Renun-A causing rock deformation, thus triggering an earthquake. In the period from July 1, 2020 to July 31, 2020, there was 1 earthquake in this fault segment. And in cluster 5 (Barumun, Angkola), Judging from the location and depth of the hypocenter, the earthquakes in this area include shallow earthquakes which are thought to be the result of the activities of the local Barumun and Angkola faults that cause rock deformation, thus triggering an earthquake. In the period 01 July 2020 to 31 July 2020, 2 earthquakes occurred in this fault segment.

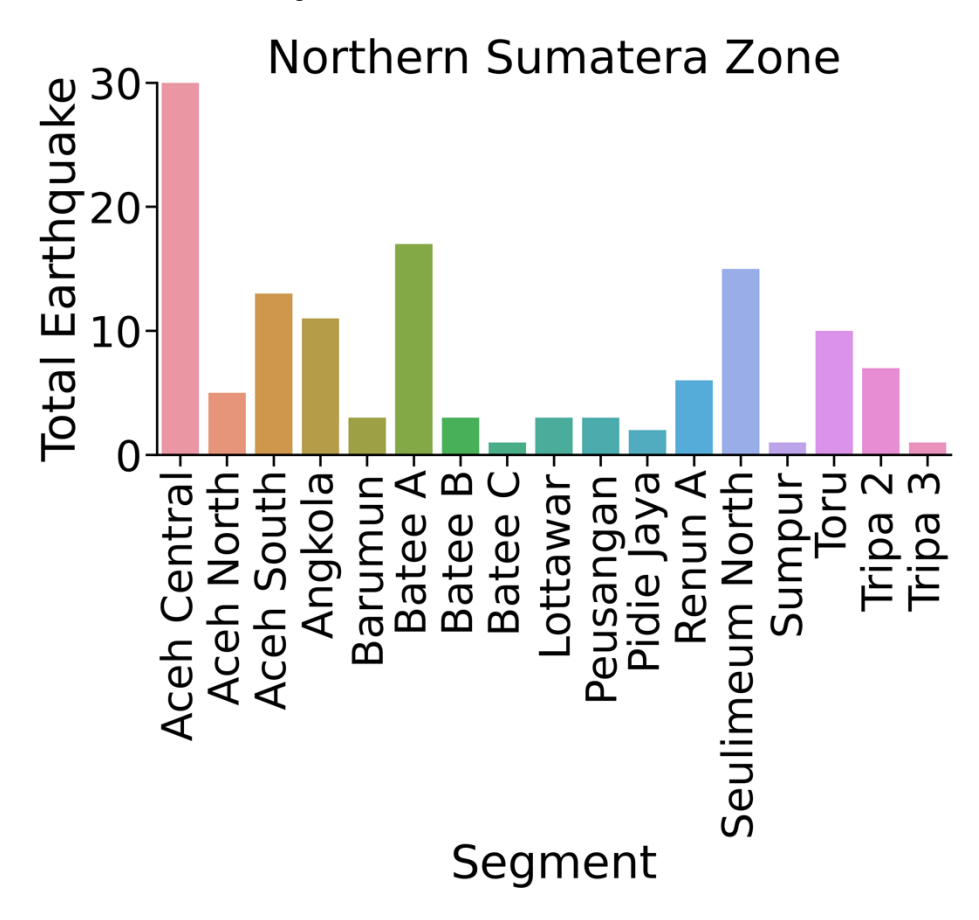


Fig.4. Segment activity analytic data in Northern Sumatra for the period January – July 2020

From the results of the study in July 2020, there was an increase in the activity of the Aceh Central segment from January-June 2020. The increase in earthquake activity in the Aceh Central segment increased by 12 times, bringing the total earthquakes in the Aceh Central segment to 31 events for the period January July 2020. Analytical data in this study, it can be seen in Figure 5. The local segment in the North Sumatra region itself which is affected by the Toru, Angkola and Renun fault segments/faults in the July 2020 study was reduced.

4. CONCLUSION

Based on the analysis that has been carried out, it can be concluded that, in the period from July 1, 2020 to July 31, 2020, there have been 79 earthquakes in the North Sumatra region, with magnitudes between 2.0 - 5.2. The location of the earthquake was dominated by land earthquakes with shallow depths, namely 0-

60 km with 54 events and at sea 25 occurrences. The most earthquake occurrences in the period 01 July 2020 - 31 July 2020 occurred around Cluster 1 (local fault Aceh Central, Batee-A, Aceh South, Pidie Jaya and Lot Aceh North, Seulimeum-South), namely 15 earthquake events, so it is classified as a cluster. which is very active in the July 2020 period. In the July 2020 period, seismic activity around the Tripa 2 and Oreng local faults was low compared to other local faults in Northern Sumatra, while in June 2020 there was no seismic activity around the Tripa local faults. 2, and the Oreng fault, so that this fault needs to be watched out for. Broadly speaking, the occurrence of earthquakes in an area indicates that the fault activity in the area is active, so it is necessary to pay attention to especially the relatively 'silent' areas located between active faults because the possibility of a strong earthquake is getting bigger.

REFERENCE

- [1] L. Prawirodirdjo *et al.*, "One century of tectonic deformation along the Sumatran fault from triangulation and Global Positioning System surveys," *J. Geophys. Res. Solid Earth*, vol. 105, no. B12, pp. 28343–28361, 2000, doi: 10.1029/2000jb900150.
- [2] C. Subarya *et al.*, "Plate-boundary deformation associated with the great Sumatra-Andaman earthquake," *Nature*, vol. 440, no. 7080, pp. 46–51, 2006, doi: 10.1038/nature04522.
- [3] R. W. Briggs *et al.*, "Deformation and slip along the Sunda megathrust in the great 2005 Nias-Simeulue earthquake," *Science* (80-.)., vol. 311, no. 5769, pp. 1897–1901, 2006, doi: 10.1126/science.1122602.
- [4] N. Earthquake et al., "Deformation and Slip Along the," Science (80-.)., vol. 311, no. March, pp. 1897–1901, 2006, doi: 10.1126/science.1122602.
- [5] P. W. Burton and T. R. Hall, "Segmentation of the Sumatran fault," Geophys. Res. Lett., vol. 41, no. 12, pp. 4149–4158, 2014, doi: 10.1002/2014GL060242.
- [6] Sinambela, "Wajah Tektonik Sumatera Bagian Utara," https://books.google.co.id/books/about?id=yyPsDwAAQBAJ&redir_esc=y, 2020. .
- [7] D. H. NATAWIDJAJA and W. TRIYOSO, "the Sumatran Fault Zone From Source To Hazard," J. Earthq. Tsunami, vol. 01, no. 01, pp. 21–47, 2007, doi: 10.1142/s1793431107000031.
- [8] H. A. Haridhi, B. S. Huang, K. L. Wen, D. Denzema, R. Agung Prasetyo, and C. S. Lee, "A study of large earthquake sequences in the Sumatra subduction zone and its possible implications," *Terr. Atmos. Ocean. Sci.*, vol. 29, no. 6, pp. 635–652, 2018, doi: 10.3319/TAO.2018.08.22.01.
- [9] M. Simoes, J. P. Avouac, R. Cattin, and P. Henry, "The Sumatra subduction zone: A case for a locked fault zone extending into the mantle," *J. Geophys. Res. Solid Earth*, vol. 109, no. 10, 2004, doi: 10.1029/2003JB002958.
- [10] M. Sinambela, M. Situmorang, K. Tarigan, S. Humaidi, and M. Sirait, "Waveforms Classification of Northern Sumatera Earthquakes for New Mini Region Stations Using Support Vector Machine," *Int. J. Adv. Sci. Eng. Inf. Technol.*, vol. 11, no. 2, pp. 489–494, 2021, doi: 10.18517/ijaseit.11.2.12503.
- [11] E. Darnila, K. Tarigan, Sunardi, F. G. Nafiri Larosa, and M. Sinambela, "Cluster analysis and seismicity partioning for northern sumatera using machine learning approach," *J. Theor. Appl. Inf. Technol.*, vol. 99, no. 2, pp. 370–380, 2021.

Time Series Forecasting for Average Temperature with the Long Short-Term Memory Network in Deli Serdang Geophysics Station

Nora Valencia Sinaga¹, Feriomex Hutagalung², Martha Manurung³, Eva Darnila⁴

^{1, 2, 3}Indonesian Agency for Meteorological, Climatological and Geophysics ⁴Department of Informatics, Universitas Malikussaleh, Lhokseumawe

Article Info

Article history:

Received September 15, 2021 Revised September 25, 2021 Accepted October 01, 2021

Keywords:

Forecasting, LSTM, Average Temperature

ABSTRACT

An understanding of trends analysis, and prediction of time series of average temperature as one of parameter weather and climate data for climate variables. It is the central process in assessing the state of the climate of a region and provides an overall estimate about the variations in the climate variables. Explore weather trends using normal and local yearly average temperatures, compare and make observations. In this study, we try to analyze local and normal average temperature data in Deli Serdang geophysc Station based on observation station in situ. The main goal of this study to compare the normal temperature to local station and to predict the average temperature data in BMKG Geophysics Station, Deli Serdang, North Sumatra using Long Short-Term Memory Model (LSTM). Based on the result of normal data science of exploring temperature with local temperature correlation, we got the display of training curve, residual plot and the scatter plot are shown using these codes. Based on the temperature series data from Geophysic station, the MSE value is 0.83 and the R2 value is 0.86.

This is an open access article under the <u>CC BY-SA</u> license.



Corresponden Author:

Martha R Manurung

Badan Meteorologi Klimatologi dan Geofisika, Indonesia

Email: naficero7@yahoo.com

1. INTRODUCTION

Climate change is currently one of humanity's most pressing issues, owing to the environmental consequences of increased greenhouse gas emissions, which are the result of human activity. Temperature is one of the most important meteorological variables that is linked to climatic events and used to describe the state of the atmosphere. The greenhouse effect's increase in global temperature is the primary driver of rising sea levels, decreasing snow and ice cover, and changing water precipitation trends. The creation of mathematical physical models to obtain patterns that allow for the prediction of climatic variables has led to the development of mathematical physical models to assist government and institutions in being prepared to avoid economic and human losses. Rising temperatures in Deli Serdang have had an impact on agriculture, health, and food security.

Temperature is a critical element in all aspects of climate change, and it is the most important weather factor influencing fire behavior. Heat waves are more likely to occur more frequently and persist longer when temperatures rise. Warmer temperatures can potentially trigger a cascade of additional global changes [1], [2]. Because rising air temperatures affect the oceans, weather patterns, snow and ice, as well as plants and animals, it's a win-win situation. We evaluated the temperature average timeseries gathered from single station in BMKG Geophysics station, Deli Serdang North Sumatra, in this study. The primary purpose of this research is to examine intermediate variables, evaluate, and forecast temperature average timeseries from 2008 to 2020. If the time series were available, the LSTM model with/without intermediate variable performed better.

In general, the findings of this study will show how average temperature can be validated and predicted as a parameter in climate data in the Medan area based on each station, and can be used as a reference in further analysis of climate data sources that can be monitored by network climate in the Medan area based

on the local observation that is the source. The purpose of this study is to compare the normal temperature to local station and to predict the average temperature data in BMKG Geophysics Station, Deli Serdang, North Sumatra using Long Short-Term Memory Model.

2. DATA AND METHOD

We used temperature data from the BMKG Geophysics Station, Deli Serdang climate library for this investigation. The temperature data was collected from 2008 to 2020, using the average temperature for Deli Serdang as the category. The temperature series data selection gives a solid foundation for analyzing the performance of observed that have been installed and examined in earlier reports. Table 1 shows a list of the temperatures recorded at each site.

Table 1. List of the Station in BMKG Geophysics Station

| No | Latitude | Longitude | Code Station |
|----|----------|-----------|--------------|
| 1 | 3.5 | 98.56 | TSI |

As in a prior study [3]–[5], we focused on analyzing temperature data as time series recorded from each station in the Medan area and using LSTM to train, test, and forecast the time series.

Figure 1, to summarize, the LSTM cell's input is a time series set of data x that runs through many sigmoid activation gates σ . To determine the cell states, each gate calculates a certain function. We merely gave a very brief overview of how LSTM works. It is still much better to take a deep learning program to learn more about LSTM. The input gate controls the flow of input activations into the memory cell, the output gate controls the cell activation flow, and the forget gate filters the information from the input and previous output and chooses which one should be remembered or not. Aside from the three gates, the LSTM cell has a cell update layer, which is normally part of the cell state. Three variables enter each LSTM cell: the current input x_t , the previous output h_t -1, and the previous cell state c_t -1. On the other hand, two variables emerge from each LSTM cell: the current output ht and the current cell state c_t .

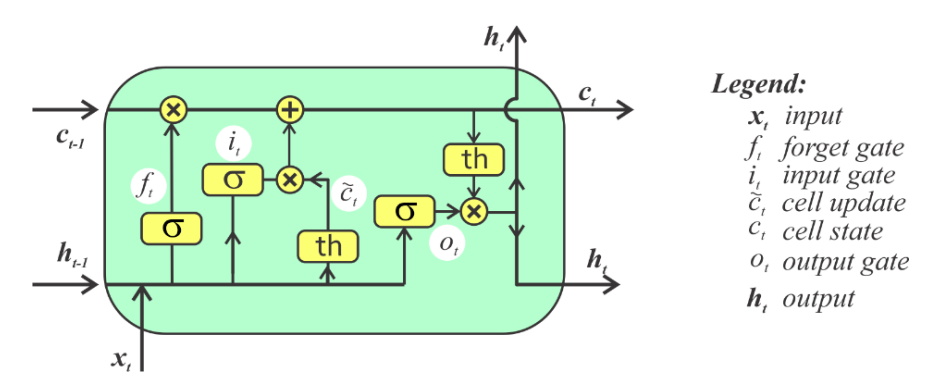


Fig. 1. The LSTM Model [6]

The current output ht computation is the LSTM cell's final stage. The current output is calculated by multiplying the output gate layer and the \tanh layer of the current cell state C_t by otimes. The current output ht has traveled through the network as either the prior state for the next LSTM cell or the input for the neural network output layer. The concepts of mean squared error and R-squared will be covered in this section. The average of the sum of squared differences between the actual value and the projected or estimated value is the mean squared error (MSE). Mean squared deviation is another name for it (MSD). This is how it is mathematically represented [7].

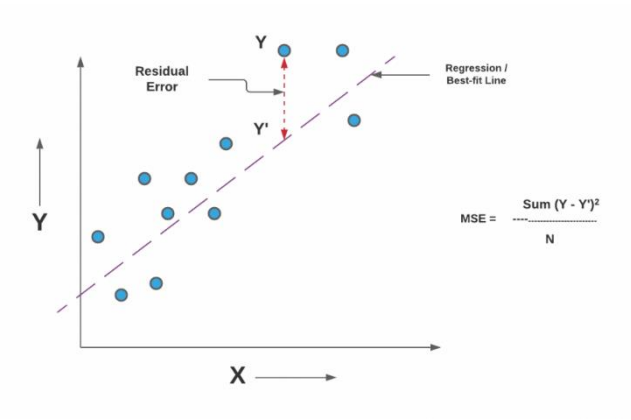


Fig. 2. Mean Squared Error Representation [7]

MSE is always positive or larger than zero in value. A number around 0 indicates that the estimator / predictor is of higher quality (regression model). The fact that the predictor has an MSE of zero (0) indicates that it is a perfect predictor. When the MSE value is squared, the result is root mean squared error (RMSE). The actual value is represented by Y, while the anticipated value is represented by Y' in the above equation. The diagrammatic representation of MSE [7] is shown below.

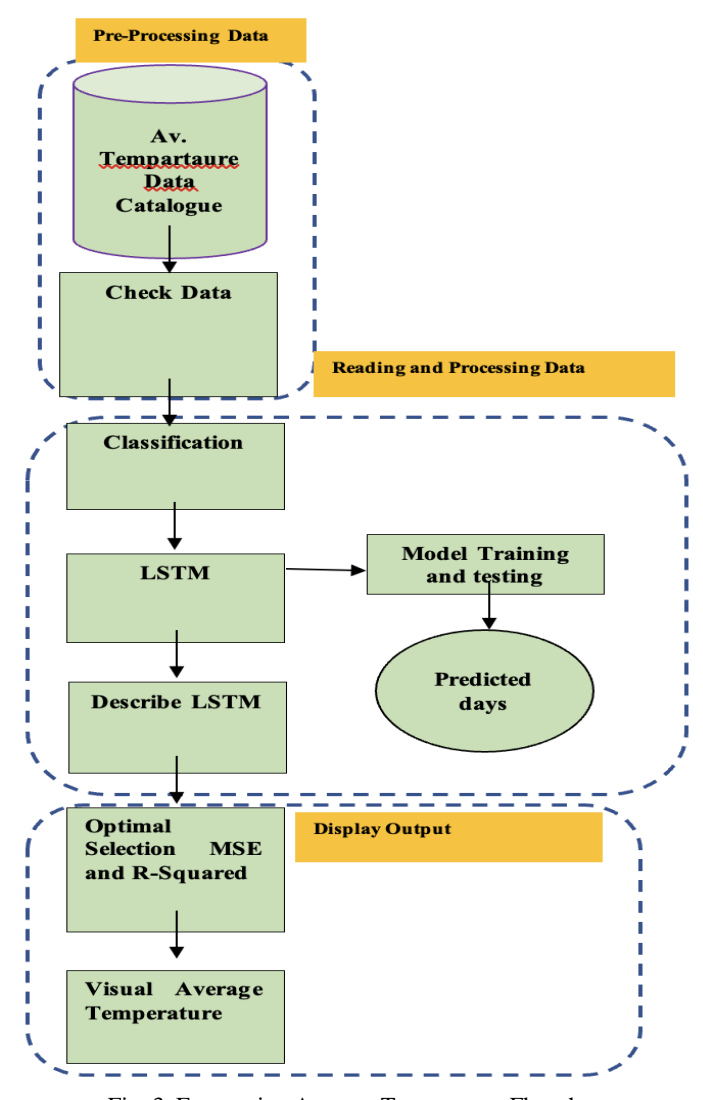


Fig. 3. Forecasting Average Temperature Flowchart

3. RESULT AND DISCUSSION

The original average temperature data was computed to ensure that our model prediction was correct. However, the projected (n days) shows that the inaccuracies are frequently caused by an unexpected surge or drop in the data, as seen in days 350-360. However, the model can correctly follow the data trend based on the first 75 days. Figure 4 depicts a graphic representation of all data from synoptic BMKG Geophysics Deli Serdang (Id Station 96037). Based on the temperature series data from Geophysic station, the MSE value is 0.83 and the R2 value is 0.86.

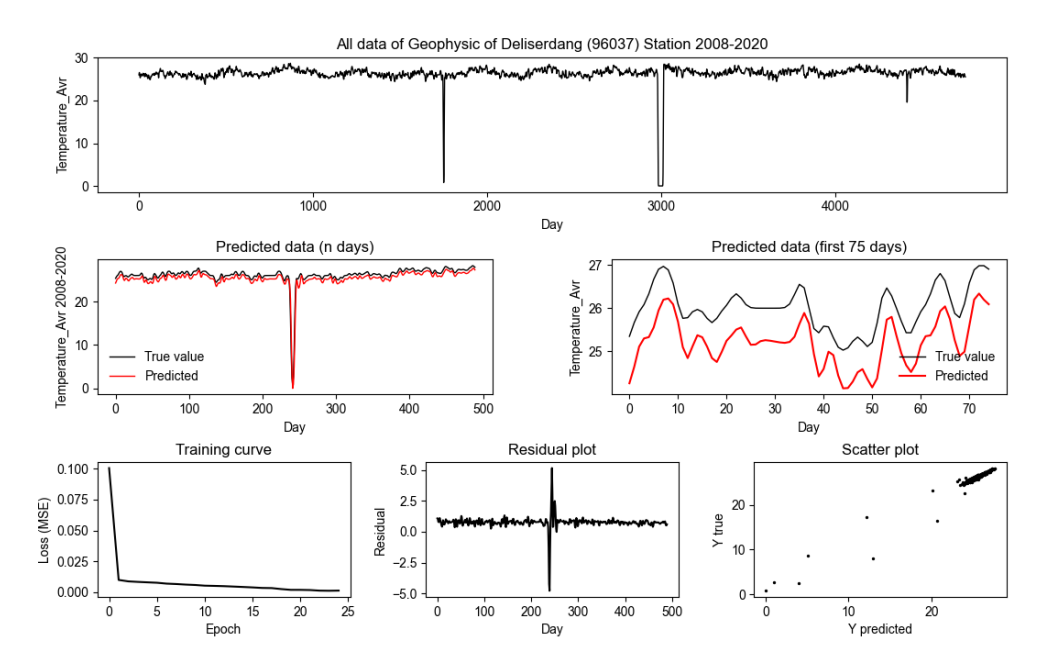


Fig. 4. Stacked LSTM prediction results in 96037 Station

The properties of temperature in the 2008-2020 timeframe are separated into MSE and R2 values using the LSTM technique. The MSE value of 96037 is 0.83, and the R2 value is 0.83, as shown in Figure 4.

4. CONCLUSION

We discovered that LSTM is an excellent method for forecasting average temperature data in this investigation. Based on the representation of BMKG Geophysics station, a number not to close to zero indicates that the estimator / predictor is of low quality (regression model). We need to evaluate the avialbale average temperature series. However, we can see from this that there are a few things to remember as LSTM lessons. To begin with, having more input days does not necessarily imply that the model will be more accurate. Aside from that, temperature data conditioning could help improve the model's accuracy. Finally, even though we haven't demonstrated it, LSTM requires a specific amount of data to work. From there, we may envisage LSTM being utilized to forecast weather and average temperature trends.

REFERENCE

- [1] Wikepedia, "Effects of climate change Wikipedia," https://en.wikipedia.org/wiki/Effects_of_climate_change, 2021. https://en.wikipedia.org/wiki/Effects_of_climate_change (accessed Mar. 10, 2021).
- [2] NASA, "Global Warming," https://earthobservatory.nasa.gov/features/GlobalWarming, 2010. https://earthobservatory.nasa.gov/features/GlobalWarming (accessed Mar. 10, 2021).
- [3] S. Afshin, H. Fahmi, A. Alizadeh, H. Sedghi, and F. Kaveh, "Long term rainfall forecasting by integrated artificial neural network-fuzzy logic-wavelet model in karoon basin," *Sci. Res. Essays*, vol. 6, no. 6, pp. 1200–1208, 2011, doi: 10.5897/SPF10.448
- [4] M. I. Hutapea, Y. Y. Pratiwi, I. M. Sarkis, I. K. Jaya, and M. Sinambela, "Prediction of relative humidity based on long short-term memory network," AIP Conf. Proc., vol. 2221, no. March, 2020, doi: 10.1063/5.0003171.
- [5] A. G. Salman, Y. Heryadi, E. Abdurahman, and W. Suparta, "Weather forecasting using merged Long Short-Term Memory Model (LSTM) and Autoregressive Integrated Moving Average (ARIMA) Model," J. Comput. Sci., vol. 14, no. 7, pp. 930– 938, 2018, doi: 10.3844/jcssp.2018.930.938.
- [6] Stanford, "Understanding LSTM Networks,"

 https://web.stanford.edu/class/cs379c/archive/2018/class_messages_listing/content/Artificial_Neural_Network_Technology_
 Tutorials/OlahLSTM-NEURAL-NETWORK-TUTORIAL-15.pdf, pp. 1–13, 2015, [Online]. Available:
 http://colah.github.io/posts/2015-08-Understanding-LSTMs/.

[7] A. Kumar, "Mean Squared Error or R-Squared, Data Analytics," https://vitalflux.com/mean-square-error-r-squared-which-one-to-use/, 2020. https://vitalflux.com/mean-square-error-r-squared-which-one-to-use/ (accessed Mar. 10, 2021).

A Review: Prototype Gyro-Stabilizer for Buoys

Amir Aziz Al Awwabin¹, Adi Widiatmoko Wastumirad²

1, 2Undergraduate Program in Applied of Instrumentation Meteorology, Climatology Geophysics (STMKG)

Article Info

Article history:

Received September 17, 2021 Revised September 25, 2021 Accepted October 01, 2021

Keywords:

Tsunami Buoy, Gyro-Stabilizer, Buoy Stability, Tsunami Early Warning System, Marine Stability Technology.

ABSTRACT

With buoys, tsunami waves caused by underwater earthquakes can be detected. The buoy will monitor and record changes in the sea level in the ocean. Indonesia has already installed several tsunami buoys. Nine buoys were made by Indonesia, two buoys made by America, one buoy from Malaysia, and the other nine buoys donated by Germany. These buoys are placed at all points in the Indonesian seas, such as in the Sumatra, Java, Flores, Maluku, and Banda Seas, so they can assist the Meteorology, Climatology and Geophysics Agency (BMKG) in providing tsunami early warnings. But unfortunately, the tsunami buoy network was not functioning from 2012 to 2018, because it was damaged and lost. Therefore, a tool is needed to maintain the presence, function, and performance of the buoy system so that it can operate properly. A Gyro-Stabilizer device can maintain the stability of the buoy. The Gyro-Stabilizer prototype is made of a simple circuit: a DC motor with a speed of around 18000 rpm and a mechanical gyroscope. The power supply uses the same power supply used by the buoy itself. As long as the Gyro-Stabilizer keeps rotating it will maintain the orientation of the buoy and make it stable. With good buoy stability, the durability and function of the electronic components inside can be maintained because the impact force from waves or sea waves can be reduced by using this Gyro-Stabilizer.

This is an open access article under the CC BY-SA license.



Corresponden Author:

Amir Aziz Al Awwabin,

Undergraduate Program in Applied of Instrumentation Meteorology, Climatology Geophysics (STMKG)

South Tangerang City, Banten, Indonesia.

Email: amir.aziz.al.awwabin@stmkg.ac.id

1. INTRODUCTION

Early detection or early warning systems are very important when natural disasters occur. With this system, the impact of damage and losses due to natural disasters can be minimized. A weather buoy is one such warning system.

Buoys are floating devices that can detect tsunami waves caused by underwater earthquakes. The buoy will monitor and record changes in sea level in the ocean [15]. Like other types of weather stations, weather buoys measure parameters such as air temperature above the ocean surface, wind speed (steady and gusting), barometric pressure, and wind direction. Since they lie in oceans and lakes, they also measure water temperature, wave height, and dominant wave period [17]. Raw data is processed and can be logged on board the buoy and then transmitted via radio, cellular, or satellite communications to meteorological centers for use in weather forecasting and climate study. Both moored buoys and drifting buoys (drifting in the open ocean currents) are used. Fixed buoys measure the water temperature at a depth of 3 meters (9.8 ft) [9]. Many different drifting buoys exist around the world that vary in design and the location of reliable temperature sensors varies. These measurements are beamed to satellites for automated and immediate data distribution [9]. Other than their use as a source of meteorological data, their data is used within research programs, emergency response to chemical spills, legal proceedings, and engineering design [17]. Like other types of buoys, moored weather buoys can also act as navigational aid. Weather Buoy records atmospheric and chaos data. This tool works automatically and is placed in the ocean. In the Pacific Ocean, at least Currently, there are more than 50 buoys

installed by research institutes in America's atmosphere and oceans (National Oceanic and Atmospheric Administration-NOAA) since the 1980s. With these tools, we get sea surface temperature data [16].

A large network of coastal buoys near the United States is maintained by the National Data Buoy Center [13], with deployment and maintenance performed by the United States Coast Guard [14]. For South Africa, the South African Weather Service deploys and retrieves its buoys, while the Meteorological Service of New Zealand performs the same task for their country [10]. Environment Canada operates and deploys buoys for their country [19]. The Met Office in Great Britain deploys drifting buoys across both the northern and southern Atlantic oceans [20].

In Indonesia, several buoys have been installed. Nine buoys were made by Indonesia, two buoys made by America, one buoy from Malaysia, and the other nine buoys donated by Germany. These buoys are placed at all points in the Indonesian seas, such as in the Sumatra, Java, Flores, Maluku, and Banda Seas so that they can assist the Meteorology, Climatology and Geophysics Agency (BMKG) in providing tsunami early warnings. But unfortunately, the tsunami buoy network was not functioning from 2012 to 2018, because it was damaged and lost [15]. Therefore, a tool is needed to maintain the presence, function, and performance of the buoy system so that it can operate properly. In this research, the authors plan to make a Gyro-Stabilizer Prototype for buoys to maintain the stability of the buoys when they are released into the ocean. Buoy stability is the buoy's ability to return to an upright position or original position when exposed to external actions such as wind, waves, and current [1].

2. DATA AND METHOD

The solution offered is the addition of a component in the form of a gyroscope stabilizer that serves to stabilize the angle of inclination due to rolling waves [8]. The gyroscope is a device in the form of a rotating disc on its axis and generates the angular momentum that maintains its position if present outside influences [4]. In this research, the dimensions of the gyro-stabilizer prototype were adjusted according to the type of weather buoy.

Weather buoys range in diameter from 1.5–12 meters (5–40 ft). Those that are placed in shallow waters are smaller in size and moored using only chains, while those in deeper waters use a combination of chains, nylon, and buoyant polypropylene [17]. Since they do not have direct navigational significance, moored weather buoys are classed as special marks under the IALA scheme, are colored yellow, and display a yellow flashing light at night.

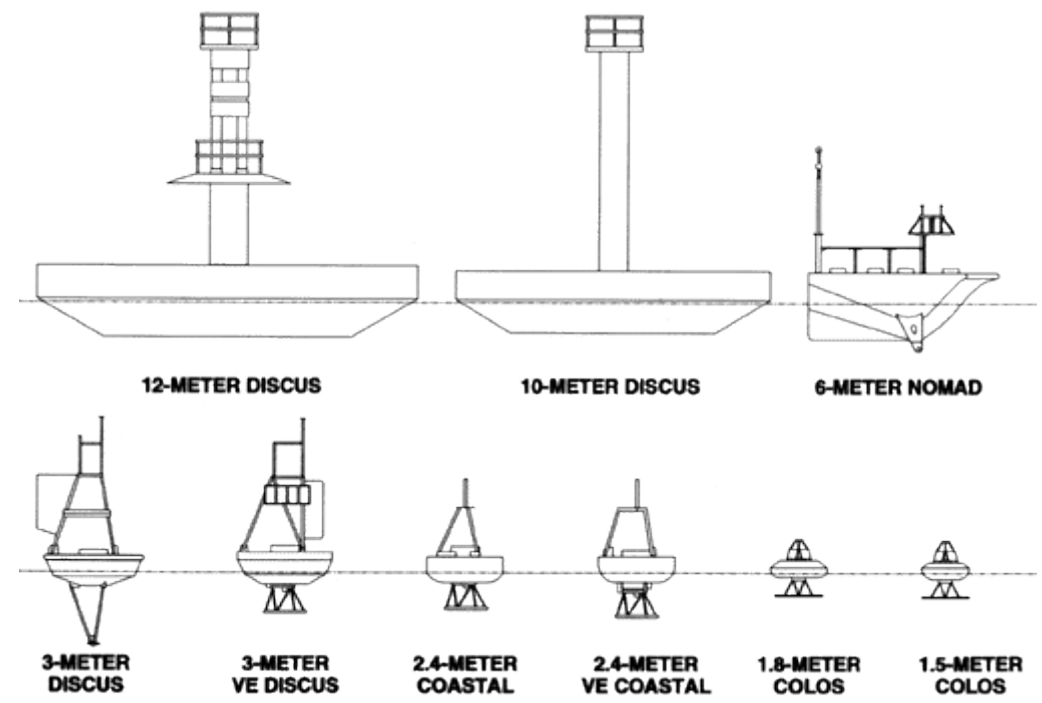


Fig 1. Types of moored buoys used by the National Data Buoy Center [17]

Discus buoys are round and moored in deep ocean locations, with a diameter of 10–12 meters (33–39 ft) [11][12]. The aluminum 33-meter (10 ft) buoy is a very rugged meteorological ocean platform that has long-term survivability. The expected service life of the 3-meter (10 ft) platform is more than 20 years and properly

maintained, these buoys have not been retired due to corrosion. The NOMAD is a unique moored aluminum environmental monitoring buoy designed for deployments in extreme conditions near the coast and across the Great Lakes [11]. NOMADs moored off the Atlantic Canadian coast commonly experience winter storms with maximum wave heights approaching 20 meters (66 ft) into the Gulf of Maine.

Drifting buoys are smaller than their moored counterparts, measuring 30–40 centimeters (12–16 in) in diameter. They are made of plastic or fiberglass and tend to be either bi-colored, with white on one half and another color on the other half of the float, or solidly black or blue. It measures a smaller subset of meteorological variables when compared to its moored counterpart, with a barometer measuring pressure in a tube on its top. They have a thermistor (metallic thermometer) on their base, and an underwater drogue, or sea anchor, located 15 meters (49 ft) below the ocean surface connected with the buoy by a long, thin tether [18].

Based on the types of weather buoys above, the authors plan to make a gyro-stabilizer prototype dimension for the type of weather buoy at 1.5 meters to 2.4 meters in size. The Gyro-Stabilizer will be built using a fixed gimbal concept. Single gimbal gyrostabilizer systems can provide larger stabilizing moments than double gimbal systems. Single gimbal gyrostabilizers transfer stabilizing moments through the gimbal structures, where the structure strength defines the maximum allowable moment. Double gimbal systems transfer the stabilizing moments through gimbal motor(s), limiting the maximum stabilizing moment to the maximum motor torque, unless the motor has some mechanical anti-backlash device, e.g., a ratchet mechanism [5].

The research method that the author uses in this study is a comparative method using a quantitative approach. Research using the comparative study method (Comparative Study) is done by comparing the equations differences as a phenomenon to find what factors/situations can cause a particular event to occur. This research begins by comparing which factors or variables are most influential to changes that occur in the results of research that is being carried out [7].

In this research, the general weather buoy prototype was used. The design of the weather buoy prototype uses a ball that is weighted in the middle of the bottom, with overall dimensions of around $1.5 \times 0.5 \times 0.5$ meters. The Gyro-Stabilizer is assembled separately from the weather buoy frame, it will be assembled in a square box with a DC motor inside. However, the gyro-stabilizer box will later be placed in the middle of the weather buoy so that the two become one part.



Fig. 2. Gyroscope Stabilizer [8]

Testing this gyro-stabilizer prototype uses the dependent variable, namely the angle of inclination of the boat which is carried out several repetitions so that the min, max, and average values are found. While variables are independent in the form of flywheel rotation speed (rpm), and wave height. To measure the tilt angle, the smartphone will be placed on top of the gyro-stabilizer box. The smartphone uses the LSM6DSL sensor in it. The LSM6DSL sensor will record the level of slope that occurs.

The LSM6DSL is a system-in-package featuring a 3D digital accelerometer and a 3D digital gyroscope performing at 0.65 mA in high-performance mode and enabling always-on low-power features for an optimal motion experience [6].

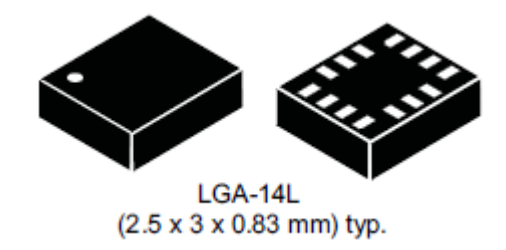


Fig. 3. LSM6DSL system-in-package

The equations of motion of a rigid body about a fixed point. Differentiating the equation $H = \sum (r x)$ mv) concerning time, we have:

$$\frac{d\mathbf{H}}{dt} = \frac{d}{dt} \Sigma (\mathbf{r} \times m\mathbf{v}) = \Sigma \left(\mathbf{r} \times m \frac{d\mathbf{v}}{dt} + \frac{d\mathbf{r}}{dt} \times m\mathbf{v} \right)$$
$$= \Sigma [(\mathbf{r} \times m\mathbf{a}) + (\mathbf{v} \times m\mathbf{v})].$$

But ma = F and $v \times v = 0$. Hence the above relation becomes:

$$\frac{d\mathbf{H}}{dt} = \Sigma(\mathbf{r} \times \mathbf{F}) = \mathbf{M}$$
 by (M= r x F)

$$= M_x \mathbf{i} + M_y \mathbf{j} + M_z \mathbf{k}, \quad \dots (1.1)$$

where M denotes the sum of the moments of all the external forces acting on the body. From (1.1) $M_x = yZ - zY$, $M_y = zX - xZ$, $M_z = xY - yX$.

$$M_x = yZ - xI$$
,
 $M_y = zX - xZ$,
 $M_z = xY - yX$.

$$\begin{split} \frac{dH_x}{dt} &= \Sigma(yZ - zY) = M_x, \\ \frac{dH_y}{dt} &= \Sigma(zX - xZ) = M_y, \\ \frac{dH_z}{dt} &= \Sigma(xY - yX) = M_z. \end{split}$$

If no external forces are acting on the body, or if there are such forces but they have no moment about the axis of rotation, then M = 0 and (1.1) becomes:

$$\frac{d\mathbf{H}}{dt} = 0.$$

Hence, $\mathbf{H} = \mathbf{a} \ \mathbf{constant} \ \dots (1.3)$ [3]

RESULT AND DISCUSSION

In this stabilization experiment, a boat prototype was used. This is due to the lack or absence of research on weather buoy stabilization using a gyro-stabilizer, however, the data generated from the stabilization of the boat tends to be relevant when paired with the use of weather buoys.

Testing of the entire system includes testing the balance of the prototype boat against given waves. The test was carried out by taking 20 samples of the slope of the prototype boat in 60 seconds and then averaging it [8].

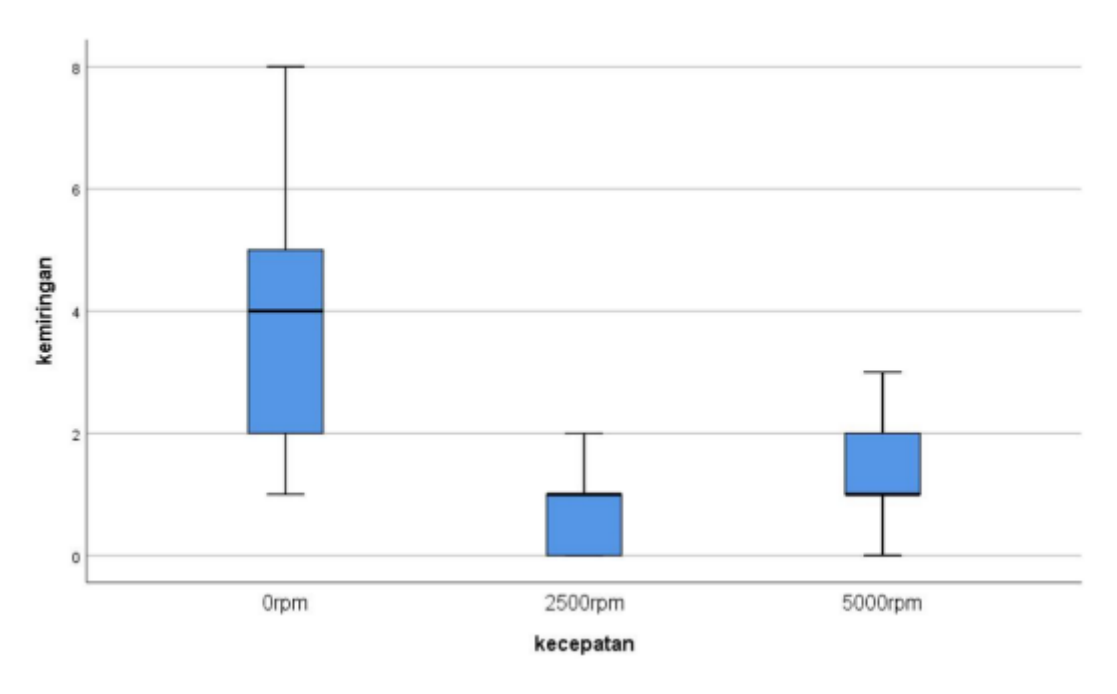


Fig. 4. Graph of test results with min, max, and average criteria [8]

The results in the figure show that without using the flywheel (0 rpm) it causes a tilt angle the highest boat in the test, when compared to the results of other tests using rotation flywheel as a stabilizer for the slope of the boat. The picture shows that at maximum rotation (500 rpm) produces a higher slope compared to medium rotation (2500 rpm) this is due to rotation which causes high vibrations on the boat structure so that the slope becomes unstable [8].

| | - | _ | - |
|------------|-----------|-----------|------------|
| | ombak 3cm | ombak 5cm | ombak 10cm |
| ──0 rpm | 2.15 | 3.75 | 5.4 |
| 2500 rpm | 0.55 | 0.9 | 1 |
| ——5000 rpm | 1.05 | 1.25 | 1.6 |

Table 1. Graph of the average boat tilt angle [8]

The graph shows the height of the waves it can produce the angle of inclination of the resulting boat. The smaller waves received by the boat, the smaller resulting slope, and vice versa. At optimal results of 2500 rpm rotation, shows the angle of inclination the lowest is at a wave height of 3 cm and a height of 5 cm and 10 cm not too far adrift, this shows that the addition of wave height provides an additional of slope that is not too large, and shows that the results achieved have been optimal in that round [8].

4. CONCLUSION

The optimal results obtained from the test show that the gyroscope stabilizer can balance the tilt angle weather buoy/boat with a range of 0.55° to 1° with a flywheel speed of 2500 rpm, and the difference in the results of the wave heights of 5 cm and 10 cm are not far apart, this shows that optimal results have been achieved even though the height is an increased wave. The test results show that the rotation on the flywheel gives good results in overcoming slope when compared to without using this tool. But if the flywheel rotation is too high can result in instability and cause vibrations to the weather buoy/boat so that it can stabilize the slope becomes less than optimal [8]. This Gyro-Stabilizer may increase the safety risk to the impact of damage caused by natural disasters such as earthquakes or hurricanes [2].

REFERENCE

- [1] E. Handayani, "Desain dan Analisis Pengaruh Penggunaan Variasi Bentuk Ballast untuk Meningkatkan Performa pada Navigation Buoy," *J. Tek. Perkapalan*, vol. 8, no. 1, p. 461, 2020.
- [2] M. Yamada, H. Higashiyama, M. Namiki, and Y. Kazao, "Active vibration control system using a gyrostabilizer," *Control Eng. Pract.*, vol. 5, no. 9, pp. 1217–1222, 1997, doi: 10.1016/S0967-0661(97)84360-2.
- [3] JAMES B. SCARBOROUGH, "The Gyroscope," p. 269, 1957.

- [4] R. A. Iswahyudi, M. Imron, and Y. Novita, "Gyroscope Sebagai Alternatif Pengganti Katir Pada Kapal Berbentuk Slender," *J. Ris. Kapal Perikan.*, vol. 1, no. 2, pp. 75–88, 2021.
- [5] N. C. Townsend and R. A. Shenoi, "Gyrostabilizer vehicular technology," Appl. Mech. Rev., vol. 64, no. 1, 2011, doi: 10.1115/1.4004837.
- [6] T. Lsm and H. Odr, "LSM6DS3 iNEMO inertial module:" no. May, pp. 1–95, 2015.
- [7] S. Bandung dan SMP Negeri, "Imay Ifdlal fahmy, 2013 Prestasi Belajar Siswa Homeschooling dan Sekolah Formal Jenjang SMP dalam Mata Pelajaran Bahasa Indonesia (Studi Deskriptif pada Homeschooling Kak BAB III METODOLOGI PENELITIAN," 2013.
- [8] D. T. Santoso, R. P. Sari, and F. F. Mudzakir, "Rancang Bangun Gyroscope Stabilizer untuk Stabilisasi Perahu," J. Rekayasa Mesin, vol. 16, no. 1, p. 62, 2021, doi: 10.32497/jrm.v16i1.2059.
- [9] W. S. Wilson and R. C. Simmons, Oceanography from space, vol. 1985-May. 1985. doi: 10.4043/4935-ms.
- [10] S. African and W. Service, "Buoy Recovery Techniques Table of Contents," pp. 1–7, 2009.
- [11] Jeff Markell, The Sailor's Weather Guide. Sheridan House, Inc, 2003.
- [12] Naval Institute Proceedings, *Watching the Oceans: A Report From General Dynamics*. Annapolis, Maryland: United States Naval Institute, 1967.
- [13] N. R. C. Lance F. Bosart, William A. Sprigg, *The meteorological buoy and Coastal Marine Automated Network for the United States*. National Academies Press, 1998.
- [14] Department of Homeland Security, "Department of Homeland Security Weather Programs," Office of the Federal Coordinator for Meteorology. p. 2, 2009.
- [15] E. Sutrisno, "Buoy, Pendeteksi Tsunami Super Cepat Buatan Indonesia," *INDONESIA.GO.ID*, 2021. https://indonesia.go.id/kategori/budaya/2543/buoy-pendeteksi-tsunami-super-cepat-buatan-indonesia (accessed Oct. 20, 2022).
- [16] BMKG RI, "BMKG (Badan Meteorologi, Klimatologi, dan Geofisika)," *Laporan Gempabumi*, 2018. https://www.bmkg.go.id/press-release/?p=bmkg-akhiri-peringatan-dini-tsunami-lombok-utara&tag=press-release&lang=ID (accessed Dec. 20, 2022).
- [17] N. D. B. C. US Department of Commerce, National Oceanic and Atmospheric Administration, National Weather Service, "NDBC Moored Buoy Program," 2015. http://www.ndbc.noaa.gov/mooredbuoy.shtml (accessed Jan. 05, 2023).
- [18] "PhOD Global Drifter Program." https://www.aoml.noaa.gov/phod/gdp/objectives.php (accessed Jan. 05, 2022).
- [19] Environment Canada, "Marine weather observations Canada," *Government of Canada*, 2010. https://www.canada.ca/en/environment-climate-change/services/general-marine-weather-information/observations.html (accessed Jan. 05, 2023).
- [20] M. Office, "Marine Observations Met Office," Met Office, 2011. http://www.metoffice.gov.uk/public/weather/marineobservations/#?tab=marineObsMap&fcTime=1479340800 (accessed Jan. 05, 2023).

A Review: Information Technology-based Climate Data Dissemination

Syalom Alfa Bazeleel Neonane¹, Adi Bagus Putrantio²

^{1, 2}Undergraduate Program in Applied of Instrumentation Meteorology, Climatology Geophysics (STMKG)

Article Info

Article history:

Received September 16, 2021 Revised September 26, 2021 Accepted October 01, 2021

Keywords:

Climate, Information, Dissemination, Application.

ABSTRACT

Changes in climate indicators can cause extreme weather and can trigger disasters, such as floods and droughts and even crop failure. it is difficult to predict because farmers and local governments do not understand the importance of climate information, the solution to the problem is to disseminate and disseminate information, but requires an information system that is also inseparable from software, IoT-based applications, and others. With the method used, namely by classifying the climate based on rainfall. In classifying the climate, the oldeman and schmidt-ferguson classifications are used. Then the dataset is formed to calculate the degree or probability of the rainfall category and the Data Normality test. The test results show that the classification of rainfall categories with light, normal, and heavy categories is 79.5%, 40.9%, and 86.4% respectively. While the precision is 96.4%, 42.6%, and 83.3% respectively. Therefore, in making applications as a medium for disseminating information, it is necessary to understand the process of seasonal occurrence, and how to turn these data into information that can be utilized by the wider community.

This is an open access article under the **CC BY-SA** license.



Corresponden Author:

Syalom Alfa Bazeleel Neonane,

Undergraduate Program in Applied of Instrumentation Meteorology, Climatology Geophysics (STMKG), South Tangerang City, Banten, Indonesia.

Email: neonanes4@gmail.com

1. INTRODUCTION

Agroclimate research and analysis often involves time series data with various time scales, ranging from hourly, daily, weekly, decadal, monthly to annual. Analysis is not only temporal but also spatial. Climate research also involves simulation models that are sometimes very complex. Dissemination and dissemination of analyzed information requires an information system that is also inseparable from the use of software, the use of open source software (OSS) is one solution in overcoming the problem of providing software[1]. Changes in climate indicators can lead to extreme weather and can trigger disasters, such as floods and droughts. One of the impacts is crop failure, which is difficult to predict because farmers and local governments do not understand the importance of climate information. One of the adaptive efforts to mitigate the effects of climate change is the holding of a Sekolah lapang Iklim (SLI), where farmers are expected to be able to apply climate information in agricultural activities [2] [3] [4] [5].

Flooding is a natural disaster that greatly disrupts community activities. Floods also cause infrastructure damage and harm economic activities. Current flood detection applications are using sensors and IOT (Internet of Things) with reports in the form of SMS (Short Message Service) gate way (Riny Sulistyowati 2015), All of these applications work in real time by utilizing current data, Machine learning can learn existing historical data patterns to predict rainfall and flooding for the next few days [6] [7]. climate / weather is a very real determinant (significant determinanr) as a factor in the instability of food production management efforts. the availability of existing rainfall data and information can be used to consider water use strategies (irrigation) in the future so that it can be utilized optimally and efficiently [8] [9].

Indonesia is a tropical region with high rainfall intensity. The use of satellite data is a widely used solution in order to reduce the gap in weather and climate information. Based on BMKG data, some data are believed to be parameters or features to be able to determine the state of the weather (rainfall). Some of the features in question include minimum temperature, maximum temperature, average humidity, length of irradiation, and wind speed [10].

Based on some of the journals above, that the application of information system technology is very important in providing climate and weather information, therefore it is necessary to understand the knowledge of current technological developments so that it can support every human activity and activity [11].

2. DATA AND METHOD

The difference in climate on earth is strongly influenced by the location of the earth against the sun, so there are several climate classifications on earth based on the geographical location of the earth, The elements of climate that show a clear pattern of diversity are the basis for climate classification. The climate element that is often used is rainfall. Climate classification is generally very specific based on its intended use, for example for agriculture, plantations, aviation, or marine [12][13].

In previous climate classification research used climate classification research using oldeman and schmidt-ferguson classifications. In climate classification using schmidt-ferguson classification is based on the comparison between dry months/*Bulan Kering* (BK) and wet months/*Bulan Basah* (BB). The provisions for determining wet and dry months follow the following rules:

Dry Month : month with rainfall less than 60mm
Wet Month : months with rainfall greater than 100mm
Humid Month : month with rainfall between 60mm-100mm

Humid months/bulan Lembab (BL) are not included in the formula for determining the type of rainfall expressed in Q values, with the following equation:

$$Q = \frac{Rata - rata \ jumlah \ BK}{Rata - rata \ jumlah \ BB} \times 100\%$$
(Schmidt, 1951)

The average number of wet months is the number of wet months of all observation data divided by the number of years of observation data, based on the magnitude of the Q value, the type of rainfall of a place or area is then determined using the Q table:

| Climate | Description | Criterion |
|-----------------|--------------|--------------------------------|
| Types | | |
| A | Very wet | 0 <q<14,3< td=""></q<14,3<> |
| В | Wet | 14,3 <q<33,3< td=""></q<33,3<> |
| С | Slightly wet | 33,3 <q<60< td=""></q<60<> |
| D | moderate | 60 <q<100< td=""></q<100<> |
| E | Slightly dry | 100 <q<167< td=""></q<167<> |
| F | dry | 167 <q<300< td=""></q<300<> |
| G | Very dry | 300 <q<700< td=""></q<700<> |
| H Extremely dry | | 700 <q< td=""></q<> |

Table 1. Schmidt-Ferguson Classification of Climate

Like the schmidt-ferguson classification, the Oldeman method (1975) also uses rainfall as the basis for climate classification.

Dry Month : rainfall smaller than 100mm
Wet Month : rainfall greater than 200mm
Humid Month : rainfall between 100-200mm

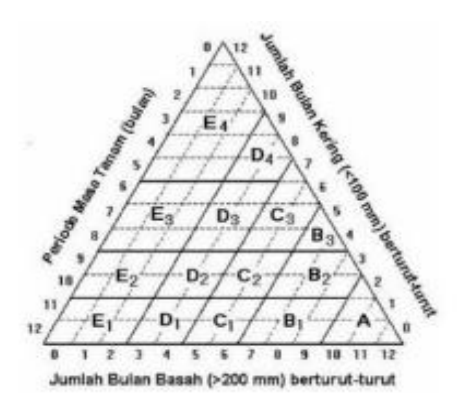


Fig 1. Oldeman's diagram (Oldeman 1975)

From the above review, Oldeman divides 5 agroclimatic regions based on water requirements, namely:

A1: wet month more than 9 consecutive months

B1: 7-9 consecutive wet months and one dry month

B2: 7-9 consecutive wet months and 2-4 dry months

C1: 5-6 consecutive wet months and 2-4 dry months

C2: 5-6 consecutive wet months and 2-4 dry months

C3: 5-6 consecutive wet months and 5-6 dry months

D1: 3-4 consecutive wet months and one dry month

D2: 3-4 consecutive wet months and 2-4 dry months

D3: 3-4 consecutive wet months and 5-6 dry months

D4: 3-4 consecutive wet months and more than 6 dry months

E1: less than 3 consecutive wet months and less than 2 dry months

E2: less than 3 consecutive wet months and 2-4 dry months

E3: less than 3 consecutive wet months and 5-6 dry months

E4: less than 3 consecutive wet months and more than 6 dry months.

3. RESULT AND DISCUSSION

The criteria F1: minimum temperature, F2: maximum temperature, F3: average humidity, F4: length of irradiation, and F5: average wind speeds are determined. In conducting this research, 150 climate data are required, namely climate data from January 2012 to December 2017 which are used as datasets. The dataset is obtained from the site http://dataonline.bmkg.go.id. Based on the dataset obtained, it is then divided into 3 parts according to the rainfall category to be classified with a composition of 50 datasets for each category [10][14].

In the dataset obtained, criteria F1 to F6 are continuous data so that the probability is calculated based on the Gauss decintas. The results of the probability calculation for all criteria are shown in the table:

Table 2. Training Data

| Non-Verbal Categories | Mean value (μ) and standard deviation (δ) | | | | | |
|----------------------------|--|-----------------|------------------|--|--|--|
| | slight | Normal | heavy | | | |
| F1:Minimum temperature | μ = 24.94 | $\mu = 23.88$ | $\mu = 23.69$ | | | |
| | $\delta = 1.35$ | $\delta = 0.75$ | $\delta = 0.815$ | | | |
| F2:Maximum temperature | $\mu = 31.41$ | $\mu = 30.46$ | $\mu = 30.15$ | | | |
| | $\delta = 1.289$ | $\delta = 1.09$ | $\delta = 1.98$ | | | |
| F3: Average humidity | $\mu = 80.38$ | $\mu = 84.84$ | $\mu = 86.2$ | | | |
| | $\delta = 4.42$ | $\delta = 4.15$ | $\delta = 4.89$ | | | |
| F4:Duration of irradiation | $\mu = 5.99$ | $\mu = 4.21$ | $\mu = 2.39$ | | | |
| | $\delta = 3.75$ | $\delta = 3.34$ | $\delta = 2.74$ | | | |
| F5: Average wind speed | $\mu = 6.92$ | $\mu = 7.68$ | $\mu = 7.72$ | | | |
| | $\delta = 2.99$ | $\delta = 3.99$ | $\delta = 3.92$ | | | |

The results of the calculation of chance statistics in Table 2 are then used to calculate the degree or probability of rainfall categories. As testing, 132 climate data are used that already know the validity of the rainfall category. Tables 3 and 4 show the testing data classification results representing each rainfall category. While table 4 shows the calculation results of light, normal and heavy rainfall classification with Naïve Bayesian [15] [7].

Table 3. The result of calculating the original data of the true category

| | CLASSIFICATION RESULT | | | | | | | |
|----------|-----------------------|--------|--------|-------|--|--|--|--|
| | | SLIGHT | NORMAL | HEAVY | | | | |
| DATA | SLIGHT | 27 | 15 | 2 | | | | |
| ORIGINAL | NORMAL | 16 | 23 | 4 | | | | |
| | HEAVY | 0 | 4 | 40 | | | | |

Table 4. The calculation results of the original data of the false category

| | CLASSIFICATION RESULT | | | | | | | |
|----------|-----------------------|--------|--------|-------|--|--|--|--|
| | | SLIGHT | NORMAL | HEAVY | | | | |
| DATA | SLIGHT | 43 | 1 | 0 | | | | |
| ORIGINAL | NORMAL | 1 | 13 | 30 | | | | |
| | HEAVY | 0 | 8 | 36 | | | | |

Table 5. Rainfall classification performance result

| PARAMETER | CATAGORY | | | | | |
|------------|----------|--------|-------|--|--|--|
| | SLIGHT | NORMAL | HEAVY | | | |
| AKURASI | 79.5% | 40.9% | 86.4% | | | |
| PRESISI | 96.4% | 42.6% | 83.3% | | | |
| RECALL | 61.4% | 52.3% | 90.9% | | | |
| ERROR RATE | 20.5% | 59.1% | 13.6% | | | |

From testing 132 data, each category of rain, light, normal and heavy 88 data. From the test results, the accuracy value for rain classification with light, normal, and heavy categories is 79.5%, 40.5% and 86.4% respectively. Based on this, the classification in normal rain conditions shows a low accuracy value. This shows the difficulty in determining the detection of normal or non-normal weather. Based on the analysis of the training data, there is no significant difference between the three categories of rain. Thus, it cannot be stated that the naive bayes approach to rainfall classification failed [16].

The Kolmogorov - Smirnov test results for the dry season cycle obtained Asympsig (2 tailed) values Dry season1 = 0.783; Dry season2 = 0.712; Dry season3 = 0.891; Dry season4 = 716; Dry season5 = 0.965; Dry season6 = 0.979; Dry season7 = 0.437; Dry season8 = 0.381. All dry season cycles have Asymp. Sig>0.05, so the residuals of the regression model are normally distributed [17] [18].

Table 6. Kolmogorov-Smirnov normality test results for the dry season cycle

Tabel 1. Hasil uji normalitasKolmogorov -Smirnov untuk siklus musim kemarau

| | | Kemarau 1 | Kemarau 2 | Kemarau 3 | Kemarau 4 | Kemarau 5 | Kemarau 6 | Kemarau 7 | Kemarau 8 |
|-----------------------------|----------------|--------------|--------------|--------------|--------------|--------------|--------------|--------------|--------------|
| N | | 10 | 10 | 10 | 10 | 10 | 10 | 10 | 10 |
| Normal Parameters* | Mean | 139.975 | 137.240 | 126.221 | 97.101 | 93.276 | 91.682 | 83.337 | 91.808 |
| | Std. Deviation | 45.225 | 49.957 | 50.868 | 34.299 | 34.479 | 41.413 | 30.158 | 36.143 |
| MostExtremeDifferences | Absolute | .207 | .221 | .183 | .221 | .158 | .149 | .275 | .287 |
| | Positive | .141 | .124 | .183 | .221 | .158 | .149 | .275 | .287 |
| | Negative | 207 | 221 | 152 | 151 | 092 | 137 | 237 | 204 |
| Kolmogorov-Smirnov Z | | .656 | .699 | .579 | .697 | .498 | .472 | .869 | .909 |
| Asymp. Sig. (2-tailed) | | .783 | .712 | .891 | .716 | .965 | .979 | .437 | .381 |
| a. Test distributionis Norm | nal. | | | | | | | | |

.

4. CONCLUSION

The test results show that the classification of rainfall categories with light, normal, and heavy categories is 79.5%, 40.9%, and 86.4% respectively. While the precision is 96.4%, 42.6%, and 83.3% respectively. Classification in light and heavy rainfall categories, the system can classify well. The possibility of low results in the normal rain category lies in the data, there should be no significant difference between the three classes. It is necessary to retest with more data [10].

The t-test results show that the dry season H0 is accepted in periods 4,5,6 and 7, meaning that there has been a change in rainfall patterns in the dry season since the period 1987 - 1996. For the wet season cycle began to be seen in the period 1995 - 2004. Although in the rainy season cycle of 1999 - 2008 t hit < t 0.975 but the value of the difference is very thin so it can be concluded that at the study site, climate change began to occur in the year of the dry season 1987 and the rainy season 1995 [17].

In understanding climate change predictions, exascale computing combined with advances in mathematical modeling and parallel algorithms will lead to new insights into the impacts of climate, including the prevalence of storms, droughts, wildfires, and more [19] [20].

From the results and discussion of several journals above, it can be concluded that in utilizing information system technology, as a determinant of seasonal rainfall data is very influential. Therefore, in making applications as a medium for disseminating information, it is necessary to understand the process of seasonality, and how to make these data into information that can be utilized by the wider community.

REFERENCE

- [1] Y. Sarvina, "Pemanfaatan Software Open Source 'R' Untuk Penelitian Agroklimat 'R' Open Source Software for Agroclimate Research," *Inform. Pertan.*, vol. 26, no. 1, pp. 23–30, 2017.
- [2] H. Subyantara *et al.*, "Penggunaan Mqtt Sebagai Optimasi Pengiriman Data Aaws Sebagai Sarana Sekolah Lapang Iklim Berbasis Internet of Things (Iot)," *J. Meteorol. Klimatologi dan Geofis.*, vol. 5, no. 1, pp. 1–10, 2018, [Online]. Available: www.mqtt.org
- [3] D. Tarmana and A. Ulfah, "Peningkatan Pemahaman Informasi Iklim Melalui Sekolah Lapang Iklim (Sli) Bagi Petani," *JMM (Jurnal Masy. Mandiri)*, vol. 5, no. 2, pp. 798–809, 2021.
- [4] I. L. Mranoto, "PERANCANGAN SISTEM INFORMASI DATA PENGAMATAN AGROKLIMAT BERBASIS WEBSITE," 2019.
- [5] N. Singh, S. Chaturvedi, and S. Akhter, "Weather Forecasting Using Machine Learning Algorithm," 2019 Int. Conf. Signal Process. Commun. ICSC 2019, pp. 171–174, 2019, doi: 10.1109/ICSC45622.2019.8938211.
- [6] I. Fitriyaningsih, Y. Basani, and L. M. Ginting, "Machine Learning: Prosperity of Rainfall, Water Discharge, and Flood With Web Application in Deli Serdang," *J. Penelit. Komun. Dan Opini Publik*, vol. 22, no. 2, 2018, doi: 10.33299/jpkop.22.2.1752.
- [7] C. J. Huang, M. C. Liu, S. S. Chu, and C. L. Cheng, "Application of machine learning techniques to Web-based intelligent learning diagnosis system," *Proc. HIS'04 4th Int. Conf. Hybrid Intell. Syst.*, pp. 242–247, 2005, doi: 10.1109/ichis.2004.25.
- [8] I. G. E. Gunartha, "APLIKASI METODE KEKERINGAN PADA PENDUGAAN DATA IKLIM/CUACA'," 1995
- [9] F. Irsyad, E. G. Ekaputra, and A. Assyaukani, "Kajian Perubahan Iklim Pada Penentuan Jadwal Tanam Cabai Di Kabupaten Agam," J. Teknol. Pertan. Andalas, vol. 23, no. 1, p. 91, 2019, doi: 10.25077/jtpa.23.1.91-102.2019.
- i gede aris gunadi, "Klasifikasi Curah Hujan di Provinsi Bali Berdasarkan Metode Naïve Bayesian," *Wahana Mat. dan Sains J. Mat. Sains, dan Pembelajarannya*, vol. 12, no. 1, pp. 14–15, 2018, [Online]. Available: https://ejournal.undiksha.ac.id/index.php/JPM/article/view/pril2018-2
- [11] E. A. Hussein, M. Ghaziasgar, C. Thron, M. Vaccari, and A. Bagula, "Basic statistical estimation outperforms machine learning in monthly prediction of seasonal climatic parameters," *Atmosphere (Basel).*, vol. 12, no. 5, 2021, doi: 10.3390/atmos12050539.
- [12] E. Gumilanggeng, "Visualisasi Informasi Klasifikasi Iklim Koppen Menggunakan Metode Polygon Thiessen (Studi Kasus Provinsi Jawa Tengah)," pp. 6–22, 2013.
- [13] A. Mihai, G. Czibula, and E. Mihuletc, "Analyzing Meteorological Data Using Unsupervised Learning Techniques," *Proc. 2019 IEEE 15th Int. Conf. Intell. Comput. Commun. Process. ICCP 2019*, pp. 529–536, 2019, doi: 10.1109/ICCP48234.2019.8959777.
- [14] A. Zakir, "Analisis dan Pengembangan Sistem Metode Prakiraan Cuaca di Bidang Informasi Meteorologi," p. 1, 2005.
- [15] Doreswamy, I. Gad, and B. R. Manjunatha, "Performance evaluation of predictive models for missing data imputation in weather data," 2017 Int. Conf. Adv. Comput. Commun. Informatics, ICACCI 2017, vol. 2017-Janua, pp. 1327–1334, 2017, doi: 10.1109/ICACCI.2017.8126025.
- [16] N. Giarsyani, "Komparasi Algoritma Machine Learning dan Deep Learning untuk Named Entity Recognition: Studi Kasus Data Kebencanaan," *Indones. J. Appl. Informatics*, vol. 4, no. 2, p. 138, 2020, doi: 10.20961/ijai.v4i2.41317.
- [17] D. Susilokarti, S. S. Arif, S. Susanto, and L. Sutiarso, "IDENTIFIKASI PERUBAHAN IKLIM BERDASARKAN DATA CURAH HUJAN DI WILAYAH SELATAN JATILUHUR KABUPATEN SUBANG, JAWA BARAT (Identification of Climate Change Based on Rainfall Data in Southern Part of Jatiluhur, Subang District, West Jawa)," *J. Agritech*, vol. 35, no. 01, p. 98, 2015, doi: 10.22146/agritech.13038.

- [18] C. He, J. Wei, Y. Song, and J. J. Luo, "Seasonal prediction of summer precipitation in the middle and lower reaches of the yangtze river valley: Comparison of machine learning and climate model predictions," *Water (Switzerland)*, vol. 13, no. 22, 2021, doi: 10.3390/w13223294.
- [19] K. Yelick, "Computing and Data Challenges in Climate Change," pp. xix-xix, 2021, doi: 10.1109/hipc50609.2020.00009.
- [20] F. Sains and U. Diponegoro, "Klasifikasi Curah Hujan di Kota Semarang Menggunakan Machine Learning Rainfall Classification in the Semarang City Using Machine Learning," vol. 1, no. 1, pp. 1–5, 2022.

Analysis of the Use of Telegram Bot for Earthquake Information Dissemination Systems and Weather Forecasting

Muhammad Bayu Putra Primary¹, Nardi²

^{1,2}Undergraduate Program in Applied of Instrumentation Meteorology, Climatology Geophysics (STMKG)

Article Info

Article history:

Received September 17, 2021 Revised September 26, 2021 Accepted October 01, 2021

Keywords:

Weather forecast, Earthquake, Dissemination, Mobile application, Telegram bot.

ABSTRACT

As one method deployment information forecast weather, BMKG has have mobile application based on Android and iOS with the name @infoBMKG since in 2016. Felt urgent for designing system with a deployment model information-based request to stay awake along with growth user application service message instant. Webhook method for Telegram Bot selected because especially effective _ for Bot creators in need guide for finish Settings base Telegram bot creation. Because of the server hosted and should use https then used Webhooks method. So, Telegram bots can respond message with fast. The success rate of Telegram Bot aimed at spreading information varies depending on the menu. A 100% success rate and an average response time of 2.54 seconds were recorded for the menu forecast weather, 100 % and an average response time of 2.76 seconds were recorded for the airport weather information menu, and 100 % and an average response time of 7.28 seconds were recorded for the image information menu satellite.

This is an open access article under the **CC BY-SA** license.



Corresponden Author:

Muhammad Bayu Putra Pratama,

Undergraduate Program in Applied of Instrumentation Meteorology, Climatology Geophysics (STMKG), South Tangerang City, Banten, Indonesia.

Email: bayu121@gmail.com

1. INTRODUCTION

The very high development of smartphone usage impacts the way communication is conducted by individuals [1]. This development can be utilized as best as possible, and the tasks within an organization can be resolved in a fast, accurate, and efficient manner [2]. According to the 2018 Digital Yearbook issued by http://wearesocial.com, it reveals that there are more than 4 billion people around the world using the internet, with the total number of internet users across continents increasing by more than 20 percent year to year. The majority of the growth in internet users over these years is driven by smartphones [3]. The use of instant messaging service applications has also continued to increase rapidly [4].

The Meteorology, Climatology, and Geophysics Agency (BMKG) is an official government institution responsible for providing public information related to weather [5]. In carrying out its duties, internet technology is very necessary for coordinating between departments or branches located throughout Indonesia [6]. This is what the BMKG is also aware of, with the use of social media rapidly growing, starting from Instagram, Twitter, Facebook, TikTok, to Telegram.

Telegram allows users to send text messages, voice messages, and communicate in groups. One of the advantages of the Telegram app compared to other similar applications is the existence of a feature in the form of an API (Application Programming Interface) available to the public [5]. As a real-time messaging application, Telegram provides convenient access for users because it is available on both mobile and desktop platforms. On the Telegram mobile platform, it can be used on iPhone, Android, and Windows Phone platforms, while on the Telegram desktop platform, it can be used on Windows, Linux, Mac OS, and also via a web browser. Telegram claims to be the fastest and safest bulk messaging application on the market. Besides that, Telegram also provides a container for developers who want to take advantage of the Open API and

Protocol, which is provided through the development of Telegram Bots, documented on the official website [1].

Weather is a very important natural phenomenon for the continuity of human life. However, weather can also cause various types of disasters, such as heavy rain, strong winds, or storms. Therefore, it is very important to have a system for disseminating weather forecasts to provide the latest information about weather conditions in a particular area. One technology that can be used to spread information about weather forecasts is chatbot applications, especially Telegram Bots. Telegram Bots allow chat application users to communicate with the system via text or voice commands. This study aims to develop a weather forecast dissemination system using Telegram Bots. This system will utilize weather forecast data available on the official BMKG website.

2. DATA AND METHOD

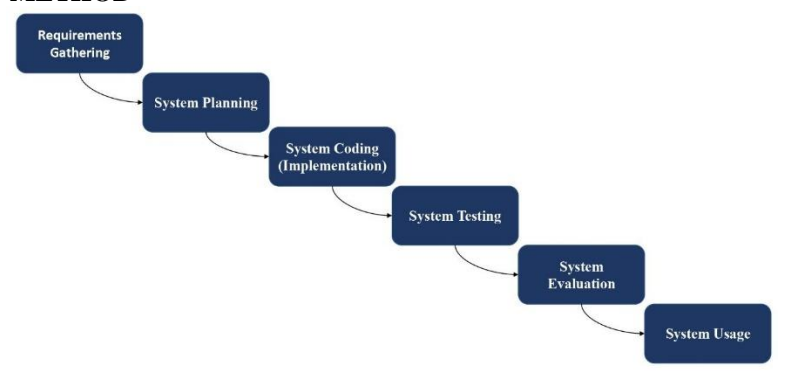


Fig 1. Prototype model

Device prototyping, or what is commonly called "soft device," is a method based on a working model with the purpose of showing the client what the system will do. This prototype is useful for understanding initial needs and determining the direction of development, as well as being a tool for designing interfaces that directly relate to user interaction. The stages of prototyping are as follows. From the prototype model image above, it can be explained as follows:

a. Collection of Needs

This stage is where customers and developers discuss the problems and needs that can be resolved by the computer system to be created.

b. Systems Planning

In this stage, system design is carried out by creating flowcharts. This stage provides details on how the system will interact with the user.

c. Coding System (Implementation)

In this step, the system that has been agreed upon by the customer and developer is translated into a programming language.

d. Testing System

In this stage, all the programs are combined into one and tested to determine whether there are any issues when the system is running. Testing can use either the white-box or black-box method.

e. Evaluation System

In this stage, the customer evaluates whether the system is running smoothly as expected, or if there are still parts that need to be repaired.

f. Use of System

In this stage, the system that has been tested is accepted by the customer and can be applied in its entirety.

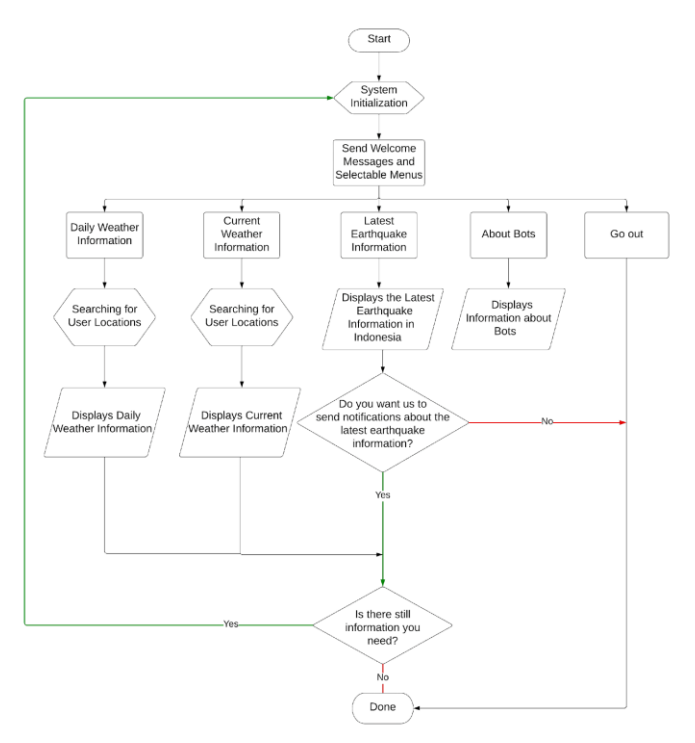


Fig 2. Diagram flow system Telegram Bots

From the flowchart, it can be understood that the process of running the Telegram bot system starts with "start," followed by "initialize system." After that, the bot will send an initial message containing the menu options provided by the bot, which includes daily weather information, current weather information, upto-date earthquake information, and information about the bot itself. Users can choose the information they need. For example, if the user selects "latest earthquake information," the Telegram bot will send the latest earthquake information to the user. Then, the bot will ask, "Would you like to receive earthquake notifications on your cellphone?" If the answer is "yes," the bot will send earthquake notifications to the user's cellphone whenever an earthquake occurs, based on the data updated on the BMKG's open data website.

If the user selects "current weather information" or "daily weather information," the bot will track the user's location using the GPS on the user's cellphone. Once the user's location is found, the Telegram bot will send either current weather information or daily weather information, according to the user's request.

Next, there is a menu about the bot itself. This menu provides information about what the bot can do. This information is the first message the bot sends when the user opens it for the first time.

The next stage occurs when the user has received the desired information—whether it is the up-to-date earthquake information, daily weather information, current weather information, or information about the bot. The bot will then ask the user, "Is there any other information you need?" If the user answers "yes," the system will repeat the process from the beginning, providing the opening message with available menu options. However, if the user wants to end the conversation with the bot, they can choose the "exit" menu, and the process will be complete.

3. RESULT AND DISCUSSION

3.1. Bot Creation

Initial process from bot creation is register the bot to be we make it on the @Botfather account with Enter the data that will be Becomes attribute on the bot later.

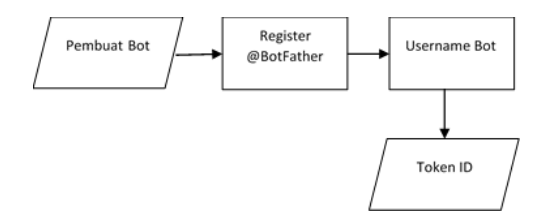


Fig. 3. Bot creation flow [5]

Then the @Botfather account will provide the IP Token which consists on code unique provided by the Telegram application. System application for Forecast Weather Info, Airport Weather and BMKG Satellite Imagery can connected with easy with using the API Token that has been provided by Telegram [5].



Fig. 4. Creating a BOT on the @Botfather account [5]

The registration process for the @BMKGbot bot account is shown in Figure 4. To start the process, enter the command /newbot in the BotFather account. After that, BotFather will respond with a request for the bot-name from the bot maker. The bot used in this investigation is called "BMKGbot". The bot-builder will respond to the message from BotFather, providing the bot's name. Once the naming procedure is done, the generated bot will be assigned a username, username@BMKGbot, as shown in the picture. After the username has been set, BotFather will send a reply message containing an embedded API Token for the bot.



Fig. 5. Appearance FIRE @BMKGbot tokens

The Telegram bot created by @BMKGbot has an API Token, which is the code that the Telegram app provides. The Telegram API token is used to connect the system application quickly for services such as Airport Weather, Weather Forecast Info, and BMKG Satellite Imagery. Each Telegram bot has a unique API Token, which can be accessed by the bot creators when needed. API tokens are also used as required based on specific needs.

3.2. Configure Webhooks

```
curl -H "Content-Type: application/json"
-X POST -d
'{"url":"https://www.[host@BMKGbot].com/h
ook.php"}'
https://api.telegram.org/bot[token@BMKGbo
t]/setWebhook
```

Fig. 6. Order Configuration Webhook @BMKGbot

Communication from servers Telegram to bot servers utilise Webhooks with protocol https. The command used for configuration Webhooks according Fig. 6 [4].

3.3. XML Data

Journal of Computation Physics and Earth Science Vol. 1, No. 2, October 2021: 54-60

```
This XML file does not appear to have any style information associated with it. The document tree is shown below.

**Cata source="meteofactory" productioncenter="NC Jakarta">
**Conceast domain="local">
**Concea
```

Fig. 7. Structure data XML for parameter

The information provided covers weather forecasts, temperature, air humidity, wind speed, and wind direction. The information is displayed for 3 days: today, tomorrow, and the day after tomorrow. Each day is divided into 4 times: morning, afternoon, evening, and early morning (the next day). The weather forecast information is taken from the XML file for each province [4].

The weather information for today is displayed using a PHP function. The parameter in the XML, as depicted in Figure 14 with ID="weather," will display the weather code for today [4].

The actual weather information from the airport that will be disseminated through the Telegram Bot application includes:

- Weather
- Temperature in Celsius
- Visibility distance in kilometers (km)
- Air pressure in hectopascals
- Wind speed in km/h
- Wind direction

To serve the actual weather information from the airport, the Telegram Bot uses PHP programming and API libraries to access BMKG Aviation XML data.

A new symbol will be added to the weather information provided at the airport to enhance the visual presentation [4].



Fig. 8. Appearance menu image satellite weather region Indonesia on application Telegram Bots

The satellite image information is collected from the Japan JMA Himawari-8 weather satellite. This Telegram Bot application presents satellite imagery based on weather conditions, categorized by region, according to Indonesian provinces. The satellite weather images are displayed as pictures with the .png extension. Telegram Bot users can request weather satellite images, which are then downloaded from the BMKG satellite server, and displayed along with weather data for the Indonesian territory covered by Himawari-8.

The results of the satellite image weather request for the Indonesian region from Himawari-8 in the Telegram Bot application are shown in Fig. 8. Users of smartphone devices have the option to zoom in and zoom out on the satellite weather images.

3.4. Application Result



Fig. 9. Appearance menu main Info BMKG weather

The current bot view system, as shown in Figure 8, initializes for the user. The bot will start the service by sending an opening message in response after the user types the command /start in the menu. The bot then replies by displaying the menu options for the user to choose from after the opening message. As mentioned before, the bot offers three menu options: Indonesian weather forecast, airport weather, and satellite imagery.

3.5. Analysis Application

Table 1. Summary Testing Bots (On Every Device)

| Category | Amount Command | Amount Testing | Level Success | Response time | Flat Flat |
|------------------|-------------------|-------------------|------------------|---------------|-----------|
| Forecast Weather | 576 | 576 | 100% | 2,16 - 3 s | 2.54 s |
| Weather Airport | 104 | 104 | 100% | 2,11 - 3.73 s | 2.76 s |
| Image Satellite | 35 | 35 | 100% | 6 - 8 s | 7,28 s |

The table shows the data for the weather forecast menu, with a total of 576 comments and 576 tests, resulting in a success rate of 100%. The response time ranges from 2.16 to 3 seconds, with an average of 2.56 seconds. For the airport weather menu, the total number of comments is 104, with 104 tests, resulting in a success rate of 100%. The response time ranges from 2.11 to 3.73 seconds, with an average of 2.76 seconds. Finally, for the satellite image menu, the total number of comments is 35, with 35 tests, resulting in a success rate of 100%. The response time ranges from 6 to 8 seconds, with an average of 7.28 seconds.

4. CONCLUSION

The success rate of the Telegram Bot aimed at spreading information varies depending on its menu. In the forecast weather menu, the total comments are 576, the total tests are 576, resulting in a success rate of 100%. The response time ranges from 2.16 to 3 seconds, with an average of 2.56 seconds. In the airport weather menu, the total comments reached 104, the total tests are 104, with a success rate of 100%. The response time ranges from 2.11 to 3.73 seconds, with an average of 2.76 seconds. Finally, in the satellite image menu, the total comments reached 35, the total tests are 35, with a success rate of 100%. The response time ranges from 6 to 8 seconds, with an average of 7.28 seconds.

REFERENCE

- [1] H. Soeroso et al., "Penggunaan Bot Telegram Sebagai Announcement System pada Intansi Pendidikan."
- [2] F. Teknologi, I. Universitas, I. Kalimantanmuhammad, A. Al, and B. Banjarmasin, "APLIKASI INFORMASI CUACA EKSTRIM DAN GEMPA BUMI," 2017.
- [3] R. Nufusula and A. Susanto, "Rancang Bangun Chat Bot Pada Server Pulsa Mengunakan Telegram Bot API Design a Chat Bot On Server Reseller Using Telegram Bots API", [Online]. Available: http://wearesocial.com
- [4] T. Istiana *et al.*, "Pengembangan Sistem Diseminasi Prakiraan Cuaca Menggunakan Aplikasi Bot Telegram dengan Metode Webhook," *Elektron Jurnal Ilmiah*, vol. 12, 2020.
- [5] Stmkg, "Jurnal Sekolah Tinggi Meteorologi Klimatologi dan Geofisika," https://jurnal.stmkg.ac.id/, 2022. https://jurnal.stmkg.ac.id/ (accessed Aug. 08, 2022).
- [6] A. Sulistyo and F. Andreas Sutanto, WARNING SYSTEM GANGGUAN KONEKTIVITAS JARINGAN PADA BMKG SEMARANG DENGAN TELEGRAM BOT. 2018.
- [7] H. Setiaji and I. v. Paputungan, "Design of Telegram Bots for Campus Information Sharing," in *IOP Conference Series: Materials Science and Engineering*, Mar. 2018, vol. 325, no. 1, doi: 10.1088/1757-899X/325/1/012005.
- [8] "SKRIPSI PERANCANGAN SISTEM PENYEBARAN INFORMASI GEMPA BUMI DAN PRAKIRAAN CUACA MENGGUNAKAN TELEGRAM BOT BERBASIS PYTHON DESIGN OF EARTHQUAKE AND

- WEATHER FORECAST INFORMATION DISSEMINATION SYSTEM USING TELEGRAM BOT WITH PYTHON BASED."
- [9] M. Anshori, A. Widya, P. Airlangga, and K. H. A. W. Hasbullah, "PENGEMBANGAN TELEGRAM BOT ENGINE MENGGUNAKAN METODE WEBHOOK DALAM RANGKA PENINGKATAN WAKTU LAYANAN E-GOVERNMENT".
- [10] H. Setiaji and I. v. Paputungan, "Design of Telegram Bots for Campus Information Sharing," in IOP Conference Series: Materials Science and Engineering, Mar. 2018, vol. 325, no. 1. doi: 10.1088/1757-899X/325/1/012005.
- [11] J. Arifin and J. Frenando, "Sistem Keamanan Pintu Rumah Berbasis Internet of Things via Pesan Telegram Home Door Security System Based on Internet of Things Through Telegram Message," *TELKA*, vol. 8, no. 1, pp. 49–59, 2022.
- [12] F. Ridaul Maulayya, M. Zainul Arifin, T. Hariono, and S. Artikel, "MENGGUNAKAN METODE LONG POLLING Info Artikel: ABSTRAK," no. 1, p. 11, 2019.
- [13] P. Guru, S. Dasar, M. Pendidikan, U. N. Surabaya, and U. Zuhdi, "Pengembangan Aplikasi Chatbot Whatsapp PENGEMBANGAN APLIKASI CHATBOT WHATSAPP MATERI PESAWAT SEDERHANA BAGI SISWA KELAS V SEKOLAH DASAR Yoga Dhamantara."
- [14] R. Hartono, N. Dery Sofya, T. Informatika, F. Teknik, and U. Teknologi Sumbawa, "DEVELOPMENT CENTER (CDC) UNIVERSITAS TEKNOLOGI SUMBAWA BERBASIS WEB," vol. 2, no. 2, 2021.
- [15] M. Anshori, A. Widya, P. Airlangga, and K. H. A. W. Hasbullah, "PENGEMBANGAN TELEGRAM BOT ENGINE MENGGUNAKAN METODE WEBHOOK DALAM RANGKA PENINGKATAN WAKTU LAYANAN E-GOVERNMENT".
- [16] "PROSEDUR STANDAR OPERASIONAL PELAKSANAAN PERINGATAN DINI,PELAPORAN,& DISEMINASI INFORMASI CUACA EKSTRIM".
- [17] B. Noor Rasad and E. Wismiana, "RANCANG BANGUN ALAT PENGAMAN KENDARAAN BERMOTOR MENGGUNAKAN APLIKASI TELEGRAM BERBASIS INTERNET OF THINGS (IoT)."
- [18] H. Salem and M. Mazzara, "ML-based Telegram bot for real estate price prediction," in *Journal of Physics: Conference Series*, Dec. 2020, vol. 1694, no. 1. doi: 10.1088/1742-6596/1694/1/012010.
- [19] T. Istiana *et al.*, "Pengembangan Sistem Diseminasi Prakiraan Cuaca Menggunakan Aplikasi Bot Telegram dengan Metode Webhook," *Elektron Jurnal Ilmiah*, vol. 12, 2020.
- [20] S. Heristian, R. A. Purnama, and A. Rafsandi, "RANCANG BANGUN ALAT CUCI TANGAN OTOMATIS DENGAN NOTIFIKASI TELEGRAM BERBASIS RASPBERRI PI," *CONTEN: Computer and Network Technology*, vol. 2, no. 1, pp. 1–7, 2022, [Online]. Available: http://ejournal.bsi.ac.id/ejurnal/index.php/ijse
- [21] K. Nalakhudin, M. Imron, M. Awiet, and W. Prasetyo, "Pemanfaatan Notifikasi Telegram Untuk Monitoring Perangkat CCTV Rumah Sakit Orthopaedi Purwokerto," *Technomedia Journal (TMJ)*, doi: 10.33050/tmj.v6i01.
- [22] S. Informasi et al., "JURNAL SAINS DAN INFORMATIKA," 2020, doi: 10.22216/jsi.v6i2.5749.
- [23] Y. Megalina, "PREDIKSI CUACA EKSTRIM DENGAN MODEL JARINGAN SYARAF TIRUAN MENGGUNAKAN PROGRAM MATLAB," 2014.